Applied Energy 207 (2017) 336–345

Contents lists available at ScienceDirect

Applied Energy

journal homepage: www.elsevier.com/locate/apenergy

A novel method on estimating the degradation and state of charge of lithium-ion batteries used for electrical vehicles

Ruixin Yang [a], Rui Xiong [a,*], Hongwen He [a], Hao Mu [a], Chun Wang [a,b]

[a] Collaborative Innovation Center of Electric Vehicles in Beijing, School of Mechanical Engineering, Beijing Institute of Technology, Beijing 100081, China
[b] School of Mechanical Engineering, Sichuan University of Science and Engineering, Zigong 643000, Sichuan, China

HIGHLIGHTS

- A three-dimensional response surface-based battery OCV model was constructed.
- A genetic algorithm is used to identify the model parameters.
- The accuracy and robustness of the proposed method are verified systematically.
- The proposed method shows high accuracy and robustness during the entire battery life.
- The proposed method can effectively improve the efficiency of on-line computation.

ARTICLE INFO

Article history:
Received 9 February 2017
Received in revised form 26 May 2017
Accepted 27 May 2017
Available online 7 June 2017

Keywords:
Electric vehicles
Battery
Capacity
State of charge
Degradation
Recognition

ABSTRACT

The accurate determination of the capacity degradation path and state of charge (SoC) is very important for the battery energy storage systems widely used in electric vehicles. This research can be summarized as follows. First, a three-dimensional response surface-based SoC-open circuit voltage (OCV) capacity method covering the entire lifetime of a battery has been constructed, which can be used to describe the battery capacity degradation characteristics and determine the corresponding SoC. Second, in order to capture the battery health state and energy state, a genetic algorithm (GA) is applied to identify the battery capacity and initial SoC based on a first-order RC model. Finally, to verify the proposed method, six experimental cases, including batteries with different aging states and with different data calculation durations, are considered. The results indicate that the maximum capacity and SoC estimation errors are less than 5.0% and 2.1%, respectively, for batteries with different aging states, which points to the high accuracy, stability and robustness of the proposed GA-based battery capacity and initial SoC estimator during the entire battery lifespan.

1. Introduction

Lithium-ion batteries are important energy storage devices that have been widely applied to various types of electric vehicles (EVs). Battery health assessment and efficient energy management are basic principles pertaining to battery application. As an electric vehicle core technology, accurate estimations of battery capacity and state of charge (SoC) are very important. Battery SoC is residual capacity and usually described by percentage. Battery capacity, defined as the maximum energy in ampere-hours that the battery can hold, is generally referred to as the maximum available capacity of the battery at the current aging level. After repeated cycling, battery capacity diminishes due to the modification of the positive and negative structural properties, growth on the solid electrolyte interface (SEI), and variation of the electrolyte chemical composition or reduction in active materials [1–3]. It is necessary to obtain an accurate estimation of battery capacity and SoC for the battery during its service life [4]. Otherwise, battery abuse including over-charging, over-discharging, or even thermal runaway may occur. Therefore, accurate and high-efficiency estimation of battery capacity and SoC can prolong battery service life and improve overall battery performance.

1.1. Review of existing estimation methods for battery capacity and SoC

With increased popularity and application of Li-ion batteries, the estimation of battery SoC has received much

* Corresponding author at: Department of Vehicle Engineering, School of Mechanical Engineering, Beijing Institute of Technology, No. 5 South Zhongguancun Street, Haidian District, Beijing 100081, China.
E-mail address: rxiong@bit.edu.cn (R. Xiong).

http://dx.doi.org/10.1016/j.apenergy.2017.05.183
0306-2619/

attention, resulting in improved estimation precision. The SoC estimation methods are summarized and evaluated in Refs. [1,2]; these methods are often divided into four types: conventional methods [3–5] (OCV, ampere-hour counting, and others), adaptive filter algorithms, learning algorithms [6] and non-linear observers [7]. The OCV based method is a simple approach to obtain the battery SOC, which is not suitable for EVs for batteries are required to have long time resting in order to reach balance. The ampere-hour counting method is also simple and general way for low-cost sensors and computing, which is often combined with other model based estimation approaches. But it has accumulated error and is hard to calibrate the initial error. The learning algorithms can be employed for SoC estimation. The disadvantages of this method are a great number of training data are needed and a lot of computations are required. The method of non-linear observers is not complex but when the system is observable the method can be used. Among these SoC estimation methods, adaptive filter algorithms are more suitable for EV application, and the methods proposed by the authors in Refs. [8–10] result in a SoC estimation error precision within 5%. However, most of the battery SoC estimation methods mentioned previously are based on a known capacity. Because battery capacity diminishes and performance degrades in an unpredictable and random manner, also the degradation paths of batteries are difficult to capture accurately. SoC estimation using a known capacity has obvious limitations to practical applications. Therefore, it is important that calibrate battery capacity on-line to estimate SoC accurately for practical applications.

Another important battery parameter is battery capacity. Capacity estimation techniques can be divided into two categories [11–14]: SoC-correlative and SoC-independent. The methods from the SoC-correlative category consider that battery capacity estimation is concerned with SoC. Ref. [15] uses the ratio of ampere-hour accumulation and SoC variation to estimate the battery capacity for the current aging condition. The relationship between battery OCV and SoC is used to calculate battery capacity in Refs. [16–18]. The advantage of this method is that fewer parameters are needed in the battery capacity estimation, because only the OCV-SoC relationship is used. The accuracy of this method is high for different aging states during the entire battery application lifespan if the cell inconsistency of the OCV-SoC relationship is very small. The disadvantage of this method is that accurately measured OCV is difficult to obtain during the entire battery service life. Therefore, this method is difficult to use on-line. A joint estimation or dual estimation method is used to estimate battery capacity and SoC concurrently, and in Refs. [3,19–23], the extended Kalman filter (EKF), in Ref. [24], the unscented Kalman filter (UKF), in Ref. [25], the particle filter (PF), in Ref. [26], the unscented particle filter (UPF) and in Ref. [27], the recursive least square (RLS) algorithms are employed. These methods can potentially estimate battery capacity accurately as the battery is modeled, and SoC is thereby estimated [2]. However, these methods performance could increase when the system and observation noise satisfy the Gaussian distribution and the model parameters are accurate. The disadvantage of these methods is that the algorithms suffer from high complexity, high computational cost and instability.

The methods that use the SoC independently can avoid the need for a complex model. In Ref. [28], the change in battery voltage is observed to estimate the battery capacity. This estimation method is suitable for identical charging conditions, but electric vehicles subject to dynamic operating conditions could be charged inconsistently with different current. Battery impedance can also reveal capacity fade of the battery current state condition [29]. In Refs. [30–34], the authors use incremental capacity analysis (ICA) and differential voltage analysis (DVA) techniques to investigate the behavior of a battery and estimate the battery capacity. These methods can estimate battery capacity accurately only for constant current charging and discharging conditions. Consequently, they cannot be used in EVs directly.

1.2. Contributions of this study

Both the capacity and the SoC are important parameters for the battery management system (BMS) in EVs. Their accurate estimations have recently been the focus of research, particularly the capacity estimation. The accessible capacity is the base of accurate battery health assessment and efficient energy management. In this paper, the three-dimensional response surface (TRS)-based SoC-OCV capacity estimator has been constructed covering the entire lifetime of a battery, based on a GA estimator for accurate estimation of battery capacity and SoC. As a state-of-the-art optimal algorithm, the GA method is able to obtain the global optimum very efficiently. Except for the SoC-OCV-capacity response surface constructed in the beginning, limited on-board data is needed to accurately determine the battery capacity and initial SoC, even during the entire battery application lifespan. Additionally, because of its high reliability and portability, the GA algorithm is expected to be more applicable in practice compared with traditional advanced estimators such as Kalman filters. For electric vehicles application, we can send a certain period of time data of driving cycles stored in BMS on-line to a powerful computer off-line or even a cloud computing platform to compute the battery capacity and SoC. Then the calculation results are returned to the BMS via a SIM card or other mediums. We use an on-line and off-line computing manner in combination to reduce computational cost of BMS.

1.3. Organization of the paper

Section 2 first describes the flow diagram of the optimization algorithm. Next, the specific computation procedure for the capacity and SoC is presented. Section 3 introduces the configuration of the battery test bench, the schedule and the results. A battery with four different aging states and two different operating conditions is analyzed in the six case studies in Section 4 before conclusions are drawn in Section 5.

2. Description of the capacity and SoC estimation approach

2.1. An equivalent circuit model of a battery

Lithium-ion battery characteristics can be described by an equivalent circuit model for different operating conditions. Plett [27] and Hu [35] have proposed several equivalent circuit models, including the simple, one-state hysteresis, enhanced self-correcting, first-order RC, first-order RC with one-state hysteresis models, etc., and Hu has presented a comparative study of the 12 equivalent circuit models. Based on their previous research experience, we consider the first-order RC model, also called a Thevenin model, as the best choice in this paper for its high model accuracy and low computational effort. The schematic diagram of the Thevenin model is presented in Fig. 1. The model equations can be expressed by:

$$\begin{cases} U_{D,k+1} = \exp(-\Delta t/\tau_D)U_{D,k} + R_D[1-\exp(-\Delta t/\tau_D)]I_k \\ U_k = U_{oc,k} - R_o I_k - U_{D,k} \end{cases} \quad (1)$$

where U_k, $U_{oc,k}$ and I_k are the battery terminal voltage, open circuit voltage and load current at time equal to k, $U_{D,k+1}$ and $U_{D,k}$ denote the voltage of the RC network at time equal to k + 1 and k, respectively, τ_D and R_D represent the time constant and polarization resistance of the RC network, and Δt represents the sampling time.

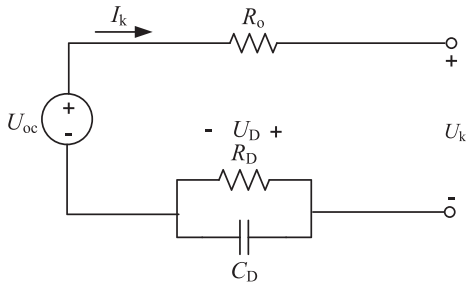

Fig. 1. The schematic diagram of the first-order RC model.

The open circuit voltage (OCV) is the voltage source of the entire circuit, and the resistor R_o represents the contact resistance of the electrode material, electrolyte, separator and other parts. R_D and C_D of the RC network describe the dynamic voltage performance of the battery which includes the diffusing effects and polarization characteristics. The time constant τ_D of the RC network can be expressed as $\tau_D = R_D C_D$.

2.2. Description of the optimization algorithm

In consideration of the convergence rate, computational memory and convenience of operation, a genetic algorithm (GA) is selected. The GA concept was introduced by Holland and his team in the 1960s and 1970s. Based on the theory of biological evolution in nature, strong and fit species tend to survive, passing their genes to the next generation by natural selection, while weak and unfit species have less opportunity to pass their genes to future offspring and are faced with extinction. The main steps in a GA are presented in Fig. 2. The figure shows that the population is normally randomly initialized with a given size and each individual of the population is a possible solution to the optimization problem. If the results do not meet the terminal condition, we calculate the fitness

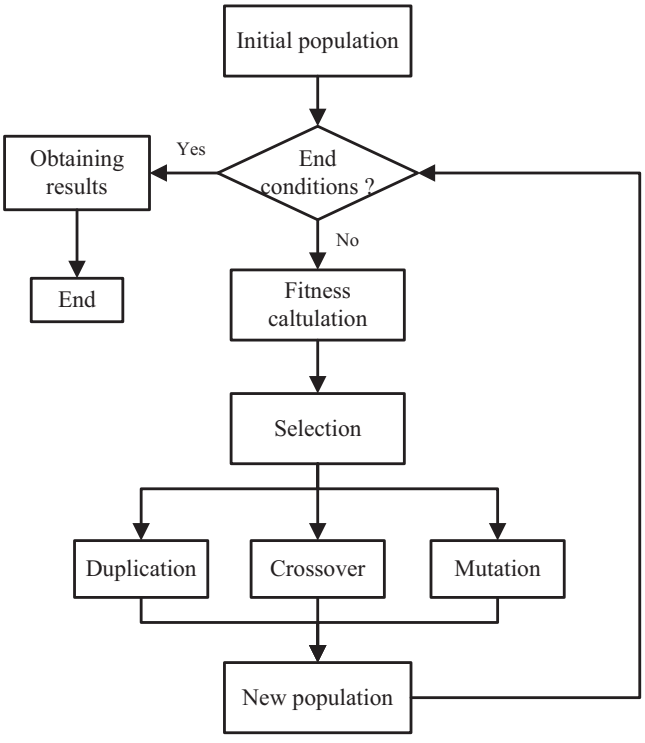

Fig. 2. Flow diagram of a GA.

of individuals and selection is made according to a certain probability. To generate new a population, duplication, crossover and mutation are necessary. If the individuals of the new population satisfy the end conditions, the calculation is terminated and the result of the optimization problem identified.

2.3. The capacity and SoC joint estimator

The proposed battery capacity and SoC estimator can be described with four steps, as shown in Fig. 3.

Step 1. Build the TRS-based OCV model.

At a certain temperature (e.g. 25 °C), the battery is repeatedly cycled. The battery OCV, SoC corresponded to OCV and battery capacity are recorded at different aging states. With the complete battery OCV data for different SoC and capacity, the TRS-based OCV model can be built. It is described by the following equation:

$$U_{oc} = f(z, Q) \tag{2}$$

where f is the battery OCV function, z is the battery SoC and Q is the battery capacity. A lithium-ion battery cell OCV versus SoC and battery capacity three-dimensional response surface is presented in Fig. 4. We hold the opinion that the TRS-based OCV model can cover the entire battery lifespan of this lithium-ion batteries type and is determined concurrently by the battery capacity and SoC.

Note that the temperature factor has been ignored in the OCV model because (1) in general, the battery system has a good battery thermal management system and the temperature deviation is maintained within ±5 °C, and (2) Fig. 7 (Section 3) shows that when the battery SoC is between 20–90%, temperature has little influence on the relationship between OCV and SoC.

Step 2. Establish the equivalent circuit model of the battery.

The Thevenin equivalent circuit model is built to describe the battery charge and discharge characteristics. It includes three parts, the voltage source OCV, the ohmic resistance R_o and the RC network, as shown in Fig. 1.

Step 3. Estimate battery capacity Q and initial SoC z_0.

During a continuous operating time T, the measured terminal voltage and (dis)charging load current are sampled. Based on the ampere-hour integral method, the battery SoC z, the initial SoC z_0 and the battery capacity Q are calculated by the following equation:

$$z = g(z_0, Q) \rightarrow g(z_0, Q) = z_0 - \frac{\int_0^t I_k d\tau}{Q} \tag{3}$$

Next, OCV-U_{oc}, battery capacity Q and initial SoC z_0 are correlated as given in

$$U_{oc} = f(z_0, Q) \tag{4}$$

When battery capacity, initial SoC and model parameters are known, we can use the model to predict battery behavior and provide an accurate SoC. These parameters are considered optimization variables χ in the GA optimization algorithm, where $\chi = [R_o, R_D, \tau_D, Q, z_0]$. The measured terminal voltage U and sampled (dis)charging load current I of the battery are substituted into the model Eq. (1), and the optimization variables χ are identified using the GA optimization algorithm method. The battery capacity Q, the initial SoC z_0 and other battery parameters are identified

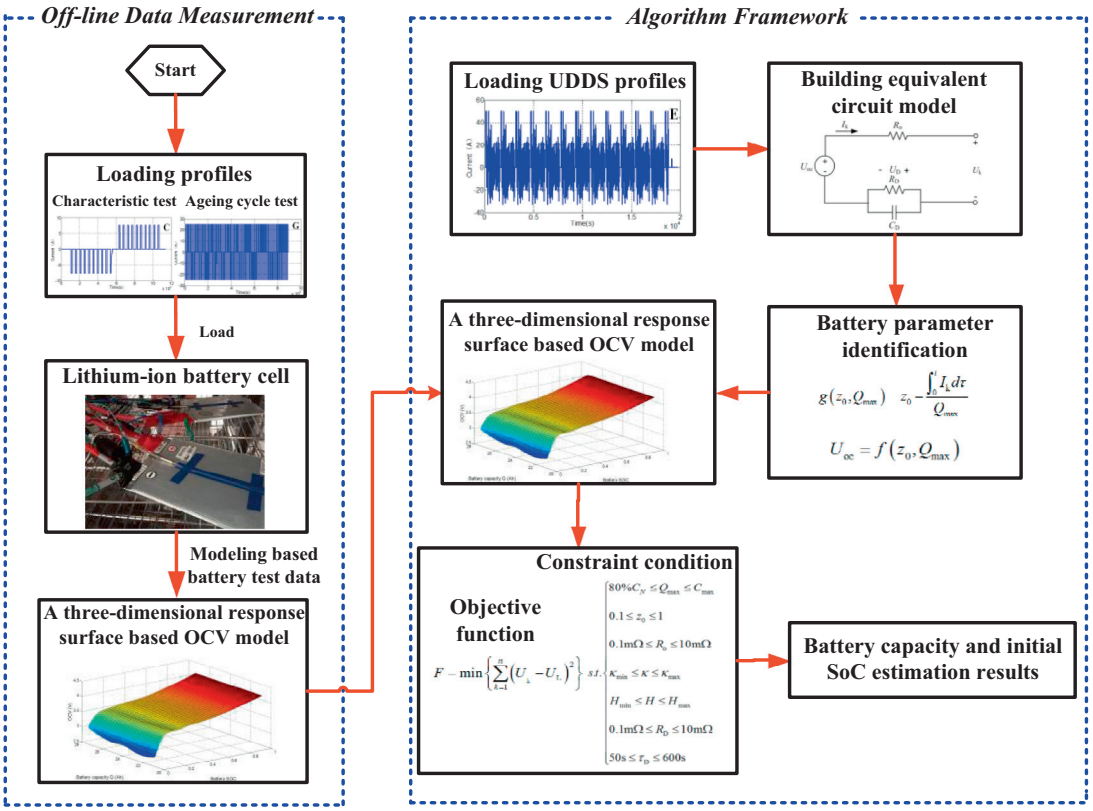

Fig. 3. A general diagram of the battery capacity and SoC estimation-based battery OCV model.

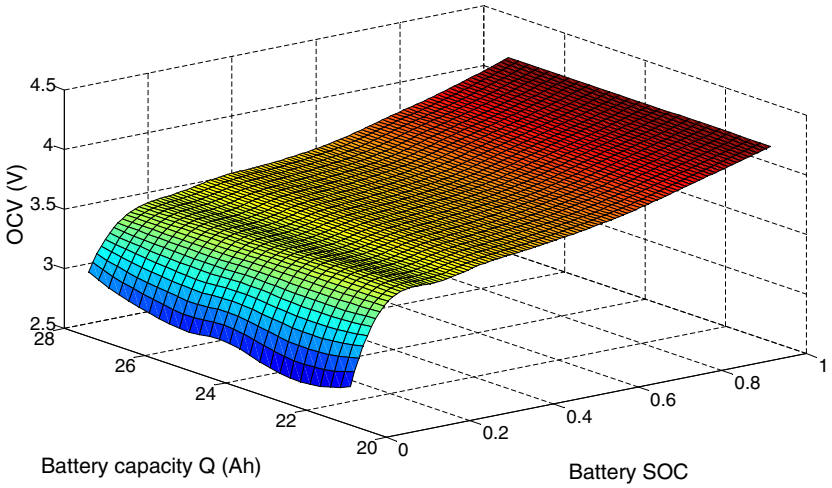

Fig. 4. A TRS-based battery OCV model.

concurrently. In the process of identification, the objective function F is the sum of the least square error between the estimated and measured voltage, as given in

$$F = \min\left\{\sum_{k=1}^{n}(U_k - U_L)^2\right\} \tag{5}$$

where U_k represents the estimated terminal voltage and U_L represents the measured terminal voltage. The sum of the least square error between the estimation and measurement is correlated to the optimum matching relationship between the OCV and the SoC of the TRS-based OCV model. The constraint conditions of the optimization algorithm are shown as

$$s.t.\begin{cases} 80\%C_N \leqslant Q \leqslant C_{max} \\ 0.1 \leqslant z_0 \leqslant 1 \\ 0.1\ \mathrm{m\Omega} \leqslant R_o \leqslant 10\ \mathrm{m\Omega} \\ \kappa_{min} \leqslant \kappa \leqslant \kappa_{max} \\ H_{min} \leqslant H \leqslant H_{max} \\ 0.1\ \mathrm{m\Omega} \leqslant R_D \leqslant 10\ \mathrm{m\Omega} \\ 50\ \mathrm{s} \leqslant \tau_D \leqslant 600\ \mathrm{s} \end{cases} \tag{6}$$

The ranges of computational parameters in the constraint condition are based on the characteristics of the battery parameters themselves and technical parameters provided by the battery manufacturers. For example, in EV applications, batteries usually reach the end of service life once their capacity is reduced to 80% of their nominal capacity and therefore, the low end of the optimization range for variable Q is 80% of the battery's nominal capacity. In addition, the minimum value for the SoC is generally not less than 20%, otherwise, the service life of the battery will be reduced. Considering the working conditions of electric vehicles, the low end of the optimization variable z_0 range is 10%. Other model parameter values are based on several battery experiments we have performed previously and some parameter values shown in Section 3.

Step 4. Estimate the battery SoC.

The battery SoC z at any time during the battery's life can be obtained based on the battery capacity Q and the initial SoC z_0 using the ampere-hour integral method, as given in

$$z = z_0 - \frac{\int_0^t I_k d\tau}{Q} \tag{7}$$

where battery capacity Q and initial SoC z_0 are initially known, and I_k is the sampling current data.

3. Experiments

An equivalent circuit model for a battery can be based upon data obtained from a variety of battery experiments. In this section, the configuration and basic principles of the battery test bench are introduced. A lithium-ion battery cell database is established, which records test data for a battery from the beginning of service to the end of its service life in an EV. This database is a basis for building an OCV model.

Table 1
Cell specification of the NCM battery.

Items	Specification
Cathode material	$Li(NiCoMn)O_2$
Anode material	Graphite
Nominal capacity	25 Ah
Allowed voltage range	2.5–4.2 V

3.1. The lithium-ion battery test system

A 25 Ah NCM material lithium-ion battery cell is tested systematically and the cell specification of it is shown in Table 1. The battery test bench is shown in Fig. 5. It consists of a battery testing system (Arbin BT2000) for charging or discharging batteries, a thermal chamber for programmable temperature control and a computer for test data storage and human-computer interaction. The range of Arbin BT2000 is 5 V–100 A, allowing it to charge or discharge a 25Ah battery cell at the maximum rate of 4C. Its sampling interval is 1 s, and the auxiliary temperature channel can gather temperature information. The programmable thermal chamber can control the temperature range from −50 °C to 120 °C with a precision of ±0.5 °C. Using the host computer, we can control an Arbin BT2000 test system using the MITS Pro software and adjust the temperature of the thermal chamber using temperature control software.

3.2. The lithium-ion battery test schedule

The battery capacity tests, OCV-SoC tests, urban dynamometer driving schedule tests (UDDS) and dynamic stress tests (DST) are executed at different battery aging states. The batteries are also repeatedly cycled. The battery OCV versus SoC and battery capacities are recorded at different aging states for a specific temperature. The battery test schedule is shown in Fig. 6.

The aging cycle test results of a lithium-ion battery cell are presented for eight cycle states of 0, 100, 200, 300, 400, 480, 550 and 600 cycles (referred to as cyc00, cyc100, cyc200, . . ., and so on). The aging cycle test results for values lower than 400 cycles is equal to that of 100 cycles, but after 400 cycles, the battery capacity diminishes to less than 90% of its nominal capacity. Considering the battery service life and experimental safety, the number of cycles tested was reduced. When 600 cycles were reached, the battery capacity diminished to 20.75 Ah and the experiment was terminated.

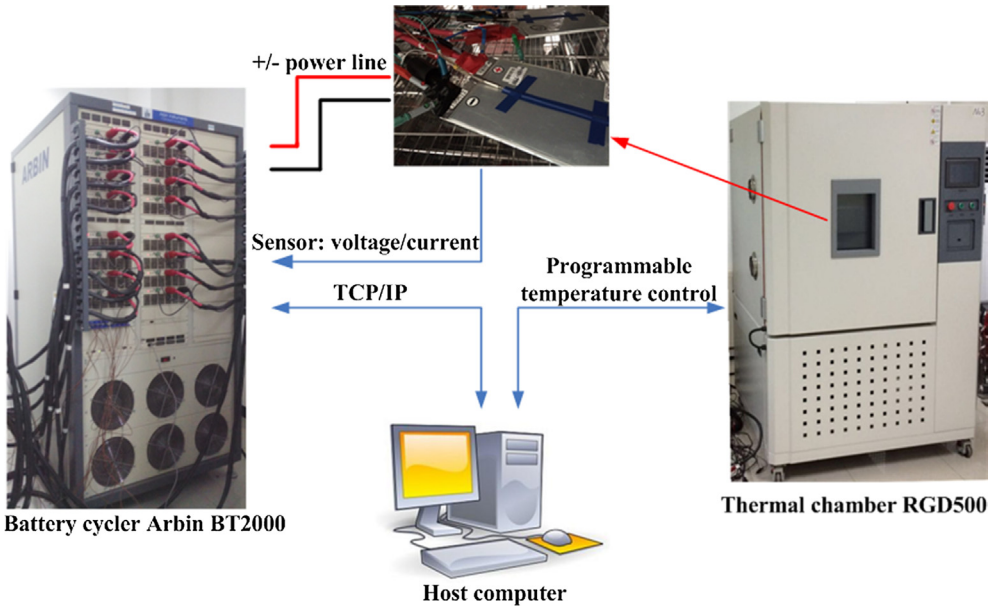

Fig. 5. Configuration of the battery test bench.

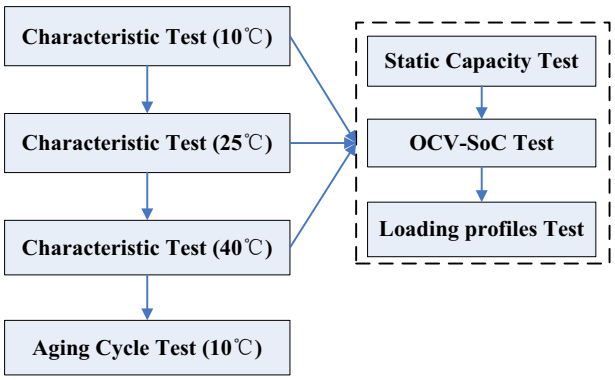

Fig. 6. The battery test schedule.

3.3. The battery test results

At temperatures of 10 °C, 25 °C and 40 °C, a 25Ah nominal capacity battery is tested with a static capacity test, an OCV-SoC test, a loading profiles test and an aging cycle test. For the static capacity test (10 °C, 25 °C, 40 °C), values for the capacity of the lithium-ion battery cell at different aging states are given in Table 2.

As Table 2 shows, with increased cycling times, the battery capacity continues to decay, dropping to nearly 80% of the nominal capacity when 600 cycles are reached. At this point, the battery should not continue to be cycle-tested and the test should be terminated.

At a temperature of 25 °C, a battery cell is tested using an OCV-SoC test for different aging states, and the resulting relationship between OCV and SoC is shown in Table 3. We list only the SoC ranges between 30–80%.

As shown in Fig. 4, the OCV model is established based on the battery capacity data and the OCV-SoC test results at the temperature of 25 °C at different aging states. As the figure shows, the battery cell OCV is determined concurrently by the battery capacity Q and the SoC. For that reason, the battery capacity Q and SoC can be used to describe the model equation and are two optimization variables in the GA algorithm.

To illustrate the influence of temperature on the relationship between battery cell OCV and SoC, the OCV-SoC test is implemented at temperatures of 10 °C and 40 °C for different aging states. The battery test results are shown in Tables 4 and 5.

Table 2
Results of a battery cell capacity test (10 °C, 25 °C, 40 °C) at different aging states.

Cycle number	cyc00	cyc100	cyc200	cyc300	cyc400	cyc480	cyc550	cyc600
Capacity at 10 °C (Ah)	25.57	24.79	24.34	24.15	23.56	22.10	20.68	20.07
Capacity at 25 °C (Ah)	27.34	25.68	25.20	24.87	24.31	22.74	21.36	20.75
Capacity at 40 °C (Ah)	27.89	25.92	25.38	25.03	24.61	23.07	21.74	20.73

Table 3
The battery cell OCV-SoC test result (25 °C) for different aging states.

cyc00		cyc100		cyc200		cyc300		cyc400		cyc480		cyc550		cyc600	
SOC	OCV	SOC	OCV	SOC	OCV	SOC	OCV	SOC	OCV	SOC	OCV	SOC	OCV	SOC	OCV
80%	3.92	80%	3.93	80%	3.93	80%	3.93	80%	3.93	80%	3.94	80%	3.94	80%	3.94
70%	3.83	70%	3.83	70%	3.83	70%	3.83	70%	3.83	70%	3.84	70%	3.85	70%	3.85
60%	3.73	60%	3.74	60%	3.74	60%	3.74	60%	3.74	60%	3.76	60%	3.77	60%	3.78
50%	3.67	50%	3.68	50%	3.68	50%	3.69	50%	3.69	50%	3.70	50%	3.71	50%	3.72
40%	3.64	40%	3.65	40%	3.65	40%	3.65	40%	3.65	40%	3.66	40%	3.67	40%	3.67
30%	3.61	30%	3.62	30%	3.61	30%	3.61	30%	3.62	30%	3.62	30%	3.62	30%	3.62

Table 4
The battery OCV-SoC test results (10 °C) for different aging states.

cyc00		cyc100		cyc200		cyc300		cyc400		cyc480		cyc550		cyc600	
SOC	OCV	SOC	OCV	SOC	OCV	SOC	OCV	SOC	OCV	SOC	OCV	SOC	OCV	SOC	OCV
80%	3.91	80%	3.92	80%	3.92	80%	3.93	80%	3.93	80%	3.93	80%	3.94	80%	3.93
70%	3.83	70%	3.83	70%	3.83	70%	3.83	70%	3.83	70%	3.84	70%	3.85	70%	3.84
60%	3.75	60%	3.74	60%	3.74	60%	3.74	60%	3.74	60%	3.76	60%	3.77	60%	3.77
50%	3.68	50%	3.68	50%	3.68	50%	3.69	50%	3.69	50%	3.70	50%	3.71	50%	3.71
40%	3.65	40%	3.65	40%	3.65	40%	3.65	40%	3.65	40%	3.66	40%	3.67	40%	3.67
30%	3.62	30%	3.62	30%	3.62	30%	3.62	30%	3.62	30%	3.62	30%	3.62	30%	3.62

Table 5
The battery OCV-SoC test results (40 °C) for different aging states.

cyc00		cyc100		cyc200		cyc300		cyc400		cyc480		cyc550		cyc600	
SOC	OCV	SOC	OCV	SOC	OCV	SOC	OCV	SOC	OCV	SOC	OCV	SOC	OCV	SOC	OCV
80%	3.92	80%	3.93	80%	3.93	80%	3.93	80%	3.94	80%	3.95	80%	3.95	80%	3.95
70%	3.82	70%	3.83	70%	3.83	70%	3.84	70%	3.84	70%	3.84	70%	3.85	70%	3.86
60%	3.73	60%	3.74	60%	3.74	60%	3.74	60%	3.75	60%	3.76	60%	3.77	60%	3.78
50%	3.67	50%	3.69	50%	3.69	50%	3.69	50%	3.69	50%	3.71	50%	3.72	50%	3.72
40%	3.64	40%	3.65	40%	3.65	40%	3.65	40%	3.65	40%	3.66	40%	3.67	40%	3.67
30%	3.61	30%	3.61	30%	3.61	30%	3.61	30%	3.61	30%	3.62	30%	3.62	30%	3.62

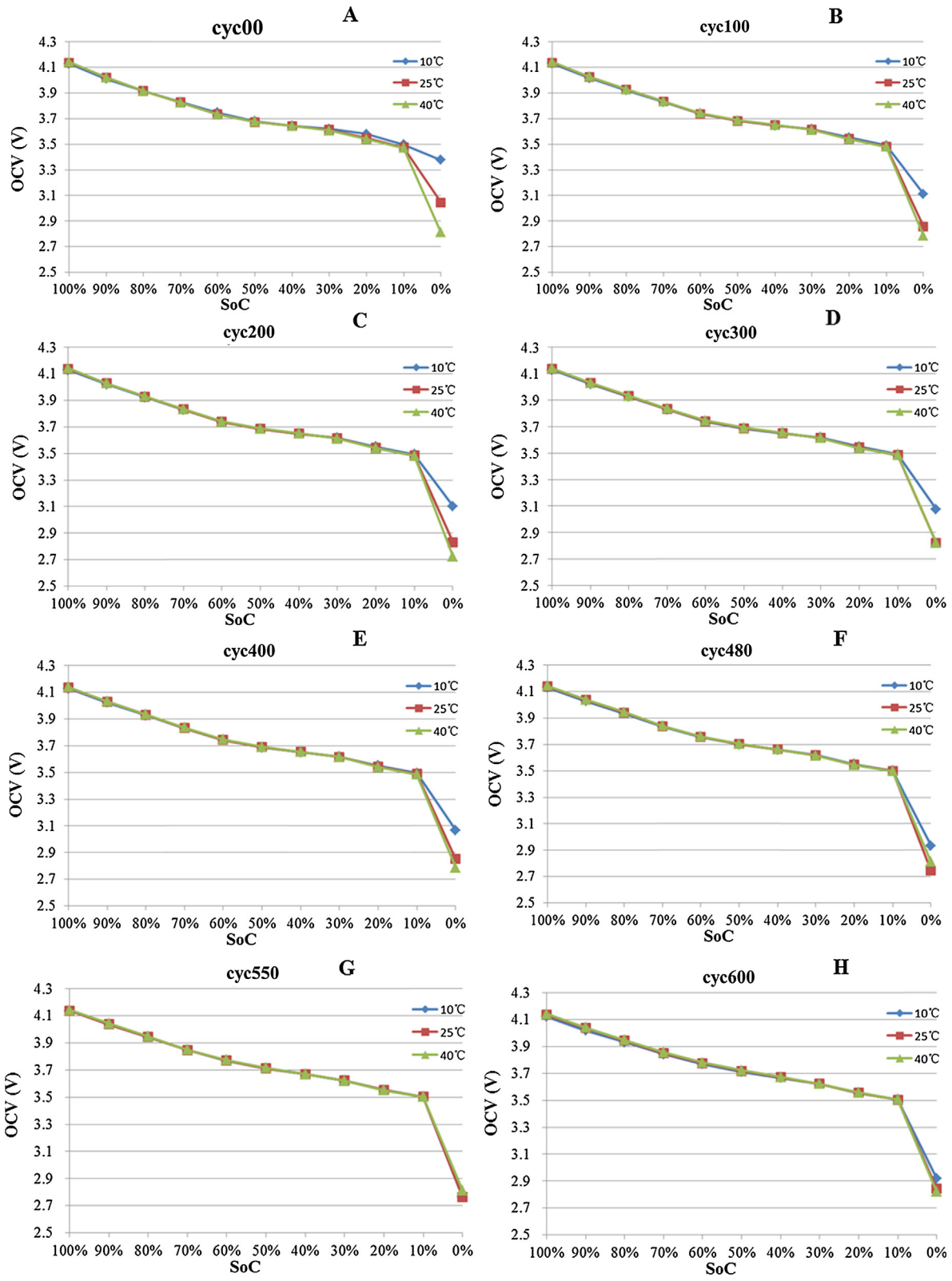

Fig. 7. The OCV versus SoC for different aging states at different temperatures.

To compare the influence of different temperatures on the relationship between OCV and SoC for different numbers of cycles, the OCV versus SoC for 10 °C, 25 °C and 40 °C are shown in Fig. 7. Parts A-H of Fig. 7 represent the OCV versus SoC for 8 different cycles-cyc00, cyc100, etc. For different numbers of cycles, the influence of temperature on the relationship between OCV and SoC is very small, especially for battery states of charge that exceed 20%.

Table 6
Description of specific details for the six cases considered.

Case number	Data length	Cycle number	Operating condition
01	3600 s	100	UDDS
02	7200 s	100	UDDS
03	3600 s	400	UDDS
04	7200 s	400	UDDS
05	7200 s	550	DST
06	7200 s	600	DST

4. Case studies

This section presents six cases to demonstrate the effectiveness of the proposed methods for battery capacity and SoC estimation for different aging states (nearly fresh battery, lightly cycled, heavily cycled and near end of service life) and different operating conditions. In case01 and case02, the battery cell has an aging level of 100 cycles and an operating condition identical to that in the UDDS test. The duration for calculating and storing data is 3600 s for case01 while the duration is 7200 s for case02. In a similar manner, in case03 and case04 the battery cell is at an aging level of 400 cycles and the same operating condition and data calculation duration as in case01 and case02 apply. In case05 and case06, the battery cell is subject to the operating conditions of the DST test and the duration of calculating and storing data is 7200 s, while the aging states are 550 and 600 cycles, respectively. Table 6 presents a clear view of the six cases considered.

We used six cases to verify stability and robustness of the battery capacity and SoC estimation method proposed in this paper with different aging states and two operation conditions (UDDS and DST). In addition, estimation accuracy influenced by different durations of data calculation is discussed using two different cases (3600 s and 7200 s).

The measured and estimated voltages versus time for the six cases are shown in Fig. 8. The figures feature a close-up view to enlarge the differences between the estimated and measured values. It is apparent that the estimated voltages trace the measured voltages closely.

The battery capacity and initial SoC estimation results for the six cases are presented in Fig. 9. The results indicate that the battery capacity estimation error is less than 5% and the battery initial SoC estimation error is less than 3%, both of which are beneficial for initial SoC calibration.

Results from Fig. 9, showing the number of cycles for cases 01–06 ranging from cyc100 to cyc600, indicate the proposed method can accurately estimate battery capacity and initial SoC for different aging states. From the estimation results, we can see that the

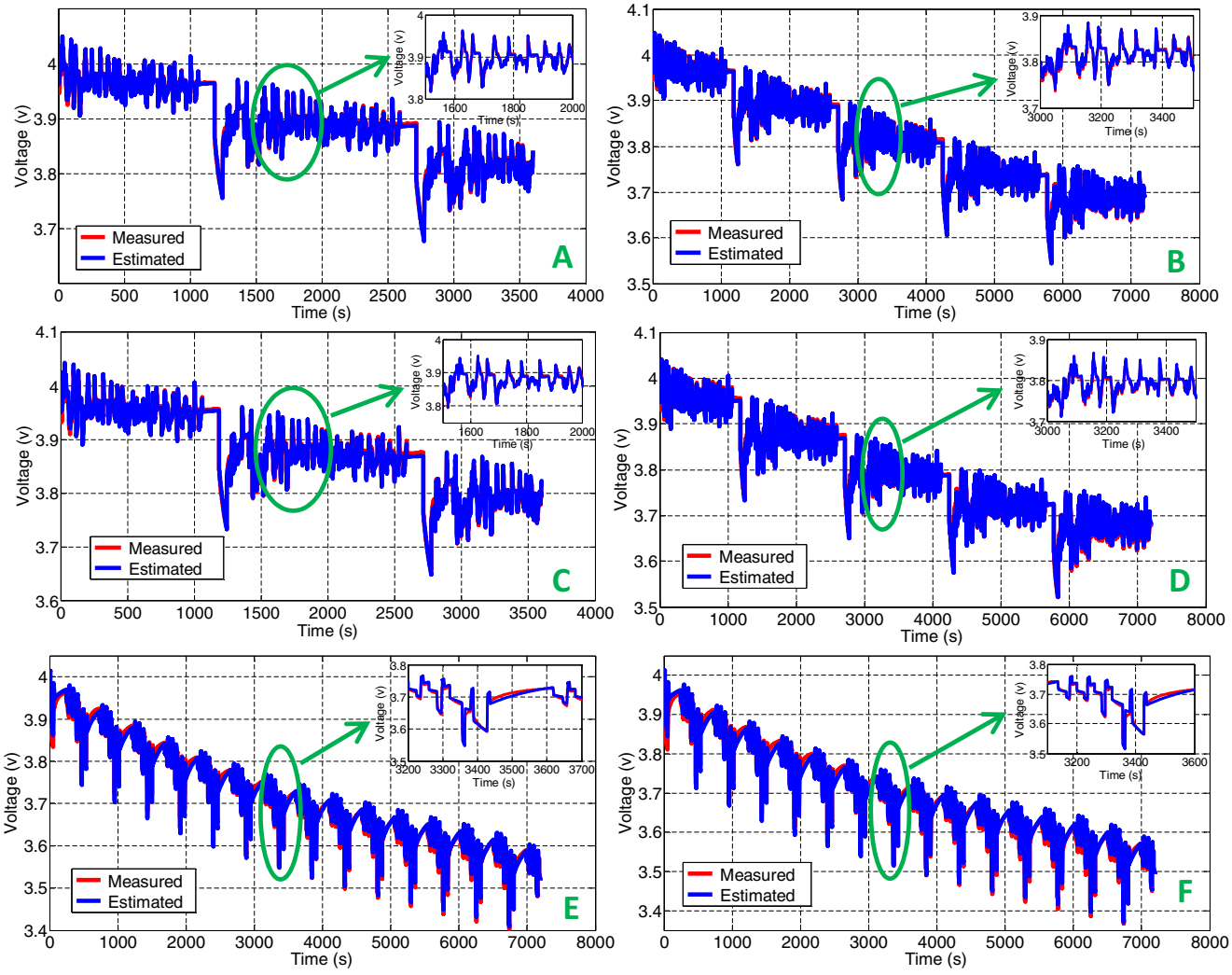

Fig. 8. Voltage versus time for six cases: A. 100 cycles and 3600 s duration (UDDS); B. 100 cycles and 7200 s duration (UDDS); C. 400 cycles and 3600 s duration (UDDS); D. 400 cycles and 7200 s duration (UDDS); E. 550 cycles and 7200 s duration (DST); F. 600 cycles and 7200 s duration (DST).

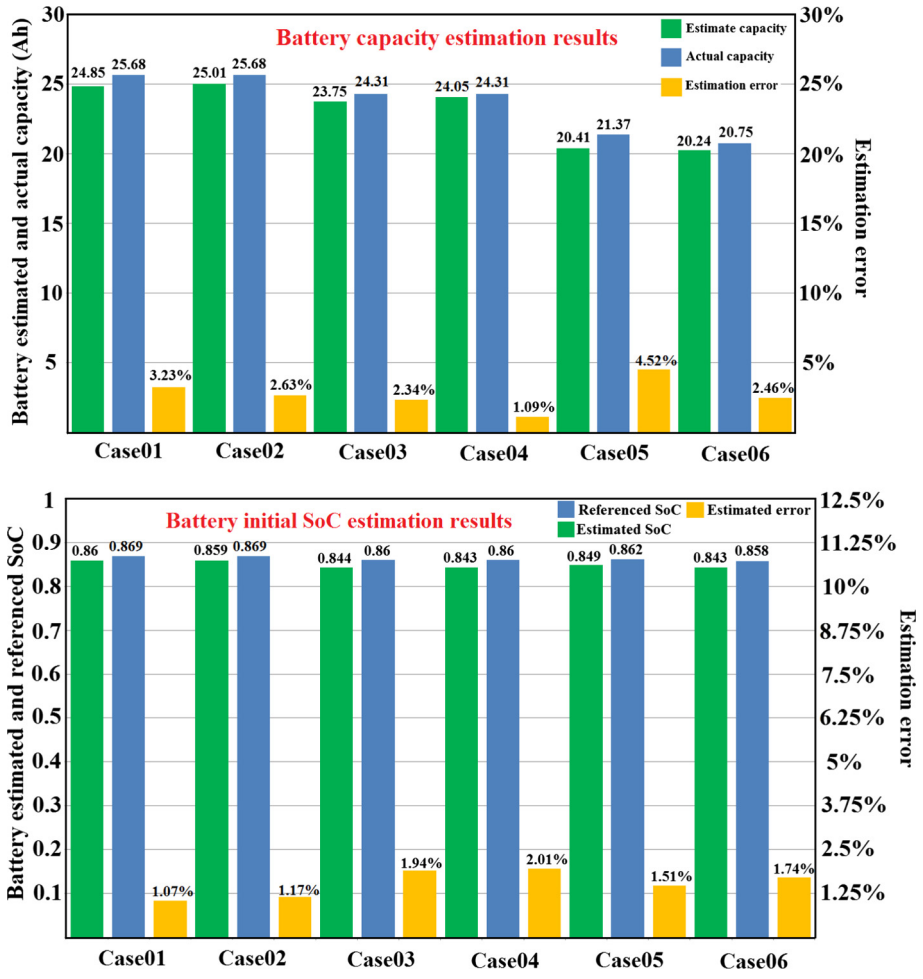

Fig. 9. Battery capacity and initial SoC estimation results for 6 cases.

estimation approach applies well to a variety of operation conditions. Comparing the results between case01 and case02 and between case03 and case04, we see how the estimation results are influenced by different durations of calculating data. From the case01 and case02 estimation results in Fig. 9, the battery capacity estimation error is reduced 0.6% from 3.23% to 2.63% while the battery initial SoC estimation error is enhanced 0.1% from 1.07% to 1.17%. The reducing and enhancing of the estimation error for case03 and case04 is similar to that of case01 and case02. In general, the battery capacity estimation accuracy is improved more than the battery SoC estimation error is increased. It is apparent that increasing the data calculation duration is beneficial to the estimation accuracy.

5. Conclusion

A battery capacity and SoC estimation approach is proposed in this paper. To verify the effectiveness of the estimation approach, many battery experiments were implemented. From the battery experiments, a battery cell test database is established, and a three-dimensional response surface-based battery OCV versus SoC battery capacity model is established for different aging states. The battery capacity and initial SoC which are taken as battery parameters are estimated using a genetic algorithm (GA) based on the Thevenin equivalent circuit model. The battery SoC and capacity are estimated. In Section 4, six cases were used to validate the reliability of the estimation approach. From the six cases, the results show that the estimation approach proposed has good robustness, stability and high accuracy for different aging states and different operation conditions, and the estimation accuracy can also be improved by increasing the time duration of data calculation.

Acknowledgments

This work was supported in part by the National Natural Science Foundation of China (Grant No. 51507012), Beijing Nova Program (Grant No. Z171100001117063), the National High Technology Research and Development Program of China (2015BAG01B01) and Joint Funds of the National Natural Science Foundation of China (Grant No. U1564206). The systemic experiments of the lithium-ion batteries were performed at the Advanced Energy Storage and Application (AESA) Group, Beijing Institute of Technology.

References

[1] Cuma MU, Koroglu T. A comprehensive review on estimation strategies used in hybrid and battery electric vehicles. Renew Sustain Energy Rev 2015;42:517–31.
[2] Xiong R, Tian JP, Mu H, Wang C. A systematic model-based degradation behavior recognition and health monitor method of lithium-ion batteries. Appl Energy 2017;207:372–83.
[3] Kong SN, Moo CS, Chen YP, Hsieh YC. Enhanced coulomb counting method for estimating state-of-charge and state-of-health of lithium-ion batteries. Appl Energy 2009;86(9):1506–11.
[4] Xiong R, Yu QQ, Wang LY, Lin C. A novel method to obtain the open circuit voltage for the state of charge of lithium ion batteries in electric vehicles by using H infinity filter. Appl Energy 2017;207:346–53.

[5] Zheng Y, Ouyang M, Lu L, Li J, Han X, Xu L, et al. Cell state-of-charge inconsistency estimation for $LiFePO_4$ battery pack in hybrid electric vehicles using mean-difference model. Appl Energy 2013;111:571–80.
[6] Charkhgard M, Farrokhi M. State-of-charge estimation for lithium-Ion batteries using neural networks and EKF. Ind Electron IEEE Trans 2011;57(12):4178–87.
[7] Quoilin S, Kawadias K, Mercier A, Pappone I, Zucker A. Quantifying self-consumption linked to solar home battery systems: statistical analysis and economic assessment. Appl Energy 2016;182:58–67.
[8] Sun F, Xiong R, He H. A systematic state-of-charge estimation framework for multi-cell battery pack in electric vehicles using bias correction technique. Appl Energy 2016;162:1399–409.
[9] Wang Y, Zhang C, Chen Z. A method for state-of-charge estimation of LiFePO4 batteries at dynamic currents and temperatures using particle filter. J Power Sources 2015;279:306–11.
[10] Zhang Y, Xiong R, He H, Shen W. A lithium-ion battery pack state of charge and state of energy estimation algorithms using a hardware-in-the-loop validation. IEEE T Power Electr 2017;32(6):4421–31.
[11] Lu L, Han X, Li J, Hua J, Ouyang M. A review on the key issues for lithium-ion battery management in electric vehicles. J Power Sources 2013;226(3):272–88.
[12] Barré A, Deguilhem B, Grolleau S, Gérard M, Suard F, Riu D. A review on lithium-ion battery ageing mechanisms and estimations for automotive applications. J Power Sources 2013;241(11):680–9.
[13] Berecibar M, Gandiaga I, Villarreal I, Omar N, Van Mierlo J, Van den Bossche P. Critical review of state of health estimation methods of Li-ion batteries for real applications. Renew Sustain Energy Rev 2015;56:572–87.
[14] Farmann A, Waag W, Marongiu A, Sauer DU. Critical review of on-board capacity estimation techniques for lithium-ion batteries in electric and hybrid electric vehicles. J Power Sources 2015;281:114–30.
[15] Waag W, Sauer DU. Adaptive estimation of the electromotive force of the lithium-ion battery after current interruption for an accurate state-of-charge and capacity determination. Appl Energy 2013;111(4):416–27.
[16] Waag W, Fleischer C, Sauer DU. Critical review of the methods for monitoring of lithium-ion batteries in electric and hybrid vehicles. J Power Sources 2014;258(14):321–39.
[17] Pop V, Bergveld HJ, Danilov D, Regtien Paul PL, Notten Peter HL. Battery management systems: accurate state-of-charge indication for battery-powered applications. London: Springer Verlag; 2008.
[18] Kessels JTBA, Rosca B, Bergveld HJ, van den Bosch PPJ. On-line battery identification for electric driving range prediction. In: IEEE Vehicle Power and Propulsion Conference (VPPC); 2011. p. 1–6.
[19] Hu C, Youn BD, Chung J. A multiscale framework with extended Kalman filter for lithium-ion battery SOC and capacity estimation. Appl Energy 2012;92(4):694–704.
[20] Xiong R, Sun F, Chen Z, He H. A data-driven multi-scale extended Kalman filtering based parameter and state estimation approach of lithium-ion polymer battery in electric vehicles. Appl Energy 2014;113(C):463–76.
[21] Lee S, Kim J, Lee J, Cho BH. State-of-charge and capacity estimation of lithium-ion battery using a new open-circuit voltage versus state-of-charge. J Power Sources 2008;185(2):1367–73.
[22] Pérez G, Garmendia M, Reynaud JF, Crego J, Viscarret U. Enhanced closed loop State of Charge estimator for lithium-ion batteries based on Extended Kalman Filter. Appl Energy 2015;155:834–45.
[23] Hu C, Youn BD, Chung J. A multiscale framework with extended Kalman filter for lithium-ion battery SOC and capacity estimation. Appl Energy 2012;92:694–704.
[24] Zhang F, Liu G, Fang L. Battery state estimation using Unscented Kalman Filter. IEEE Int Conf Robot Autom 2009:1863–8.
[25] Wang Y, Zhang C, Chen Z. A method for joint estimation of state-of-charge and available energy of $LiFePO_4$ batteries. Appl Energy 2014;135(C):81–7.
[26] He Y, Liu X, Zhang C, Chen Z. A new model for State-of-Charge (SOC) estimation for high-power Li-ion batteries. Appl Energy 2013;101(1):808–14.
[27] Plett GL. Sigma-point Kalman filtering for battery management systems of LiPB-based HEV battery packs : Part 2: Simultaneous state and parameter estimation. J Power Sources 2006;161(2):1369–84.
[28] Zheng Y, Lu L, Han X, Li J, Ouyang M. $LiFePO_4$ battery pack capacity estimation for electric vehicles based on charging cell voltage curve transformation. J Power Sources 2013;226:33–41.
[29] Waag W, Käbitz S, Sauer DU. Experimental investigation of the lithium-ion battery impedance characteristic at various conditions and aging states and its influence on the application. Appl Energy 2013;102(2):885–97.
[30] Han X, Ouyang M, Lu L, Li J. A comparative study of commercial lithium ion battery cycle life in electric vehicle: capacity loss estimation. J Power Sources 2014;268(4):658–69.
[31] Dubarry M, Truchot C, Liaw BY, Gering K, Sazhin S, Jamison D, et al. Evaluation of commercial lithium-ion cells based on composite positive electrode for plug-in hybrid electric vehicle applications. Part II. Degradation mechanism under 2 C cycle aging. J Power Sources 2011;196(23):10328–35.
[32] Weng C, Cui Y, Sun J, Peng H. On-board state of health monitoring of lithium-ion batteries using incremental capacity analysis with support vector regression. J Power Sources 2013;235(4):36–44.
[33] Feng X, Li J, Ouyang M, Lu L, Li J, He X. Using probability density function to evaluate the state of health of lithium-ion batteries. J Power Sources 2013;232(18):209–18.
[34] Bloom I, Walker LK, Basco JK, Abraham DP, Christophersen JP, Ho CD. Differential voltage analyses of high-power lithium-ion cells. 4. Cells containing NMC. J Power Sources 2010;195(3):877–82.
[35] Hu X, Li S, Peng H. A comparative study of equivalent circuit models for Li-ion batteries. J Power Sources 2012;198(198):359–67.